Photon correlation spectroscopy of the non-Markovian Brownian motion of spherical particles

Kohji Ohbayashi, Tomoharu Kohno, and Hiroyasu Utiyama

Faculty of Integrated Arts and Sciences, Hiroshima University, Higashisenda-machi, Hiroshima 730, Japan

(Received 24 November 1982)

The non-Markovian Brownian motion was studied by photon correlation spectroscopy on spherical particles suspended in viscous fluid. The non-Markovian property has been expected to give rise to a long-time tail proportional to $t^{-3/2}$ in the velocity correlation function and, correspondingly, a term of the form $p_{1/2}t^{1/2}$ in the argument of the exponential function of the photon correlation spectroscopy. Measurements were done on polystyrene latex spheres of 0.804-μm diameter suspended in pure water. Results of the experimental determination of the coefficient $p_{1/2}$ at three different temperatures were 0.397 ± 0.035 s$^{-1/2}$ at 32.8 °C, 0.326 ± 0.029 s$^{-1/2}$ at 28.0 °C, and 0.267 ± 0.027 s$^{-1/2}$ at 23.5 °C, the corresponding theoretical values being 0.409, 0.346, and 0.293 s$^{-1/2}$, respectively. Thus there is good agreement between the experimental values and the theoretical predictions.

I. INTRODUCTION

Alder and Wainright first found a long-time tail of the velocity correlation function in their computer simulation of the molecular dynamics and demonstrated that the tail was related to the slowly varying velocity field around the particle concerned.[1,2] Many theoretical studies have been done on the problem since then.[3] For example, it was soon shown that the memory effect of the Brownian motion can be explained by the kinetic theory and hydrodynamics, if we use a general expression of the drag force acting on the spherical particle.[4,5] If the Stokes formula is simply used for the drag force, the Brownian motion will become Markovian, Gaussian, and linear. Such a Brownian motion may be regarded as ideal. Interestingly, the typical Brownian motion is expected to be non-Markovian according to the modified theory. This is a realistic simple example of the non-ideal Brownian motion. The theoretical method to treat such non-Markovian, Gaussian, and linear Brownian motions is well established,[6] but the experimental tests on a real system were not sufficient to form a clear conclusion.

The diffusion coefficient calculated with the modified theory is exactly equal to the conventional Einstein-Stokes formula. Therefore, a direct measurement of the time dependence of the correlation function is necessary to test the validity of the modified theory. A few works have been done with this purpose. The existence of the long-time tail was verified qualitatively by neutron scattering on simple fluids.[7-9] The presence of the memory term in the drag force was demonstrated by the observation of a decay in the particle motion after acceleration by a shock wave.[10] The velocity correlation function in the natural Brownian motion was directly observed by Fedele and Kim and the long-time tail was shown much larger than that predicted from theory.[11] Feasibility of a long-time tail observation with the photon correlation method was proposed by Harris.[12] The density correlation function observable by the photon correlation method may, in fact, be simply related to the velocity correlation function. The measurements by Boon *et al.* showed the existence of the long-time tail in the photon correlation function.[13,14] Recently, a very accurate and quantitative determination of the long-time tail has been made by Paul and Pussey.[15] They obtained a definitely smaller value for the long-time tail than that predicted theoretically [about $(74 \pm 3)\%$]. Thus the long-time tail was observed by all the experiments so far published, but its magnitude did not agree with the theoretical prediction. It was not clear whether this discrepancy was due to experimental artifacts or to the neglect of some important terms in the theory.

In this paper, we report a photon correlation study of the Brownian motion of spherical particles in water. The long-time tail we observed was only a few percent smaller than the theoretical prediction. The temperature dependence of the long-time tail also agreed with theory.

II. THEORY

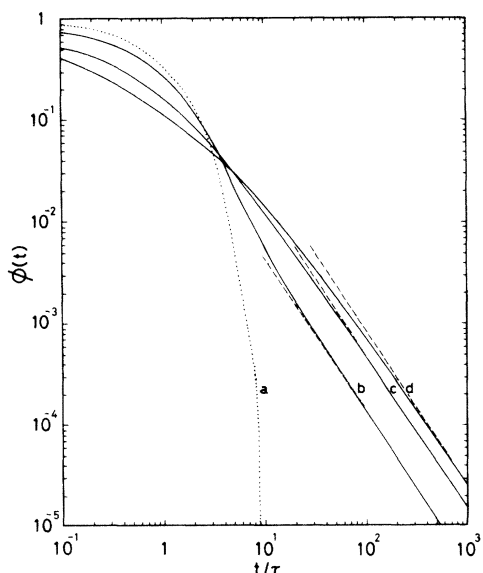The conventional theoretical model describes the dynamics of a spherical Brownian particle suspend-

FIG. 1. Normalized velocity correlation function $\phi(t)=\langle u(0)u(t)\rangle/\langle u^2\rangle$ plotted as function of the reduced time t/τ for different values of σ. Curve a, $\sigma=0$; b, $\sigma=0.477$; c, $\sigma=1.70$; d, $\sigma=3$. Broken lines are the long-time tails $(\sigma/2\pi^{1/2})(t/\pi)^{-3/2}$ for the corresponding values of σ.

ed in viscous fluid by the simple Langevin equation[16]

$$m\dot{u}(t)+\beta u(t)=f(t) , \qquad (1)$$

where $u(t)$ is the velocity of the particle at time t, m the particle mass, and $f(t)$ is the random force. The frictional coefficient β is given by the Stokes equation $\beta=6\pi a\eta$, where η and a are the viscosity of the fluid and the radius of the particle, respectively. This equation is based on the idea of Einstein.[17] The equation has been shown to be an approximation due to neglect of the effect of the fluid flow around the particle which is generated by the accelerated motion of the particle. The hydrodynamic drag force on a spherical particle moving in an arbitrary manner can be derived using the Navier-Stokes equation.[18] Then, the appropriate Langevin equation becomes[4,5]

$$m\dot{u}(t)+\beta u(t)+\tfrac{2}{3}\pi a^3\dot{u}(t)$$

$$+6a^2(\pi\eta\rho)^{1/2}\int_{-\infty}^{t}\frac{\dot{u}(t')}{(t-t')^{1/2}}dt'=f(t) . \qquad (2)$$

Here, ρ is the density of the fluid. The third term on the left-hand side is the inertia term. The fourth

term describes the effect of the accelerated fluid flow around the particle, which eventually affects the particle motion after a travel in the fluid. This term has a memory effect and the stochastic process described with this equation is thus non-Markovian. Historically, as Mazur and Bedeaux mentioned,[19] the left-hand side was derived in 1903 by Boussinesq, who extended Stokes's work. Einstein mentioned that his theory was an approximation due to the neglect of the inertia term.[17]

The velocity correlation function derived from the simple Langevin equation, Eq. (1), is

$$\langle u(0)u(t)\rangle=\langle u^2\rangle\phi(t)=\langle u^2\rangle\exp(-t/\tau) , \qquad (3)$$

where $\langle u^2\rangle=k_BT/m$ and $\tau=m/\beta$. This is a single exponential function. The derivation of the velocity correlation function from the modified equation, Eq. (2), has been discussed by many authors.[4,5,20−24] Here, we use the expression derived by Kubo[22]:

$$\langle u(0)u(t)\rangle$$

$$=\langle u^2\rangle\phi(t)$$

$$=\langle u^2\rangle\frac{1}{\pi}\int_{-\infty}^{\infty}\frac{\sigma z^2\exp(-z^2t/\tau)}{(z^2-1)^2+\sigma^2z^2}dz , \qquad (4)$$

where $\langle u^2\rangle=k_BT/m^*$, $\tau=m^*/\beta$, with $m^*=m+\tfrac{2}{3}\pi\rho a^3$, and $\sigma=[9\rho/(2\rho_0+\rho)]^{1/2}$, with ρ_0 being the density of the particle. This equation can be related to the expression derived by Widom.[5]

Equation (4) shows that the dependence of the velocity correlation function on the reduced time (t/τ) is determined solely by the dimensionless parameter σ. For usual Brownian particles, such as a polymer in water, the density of the particle is nearly equal to the density of fluid; for example, $\rho_0=1.03$ g/cm^3 for polystyrene latex spheres, and $\sigma=1.70$. Two other realistic limiting cases are a heavy particle such as gold ($\rho_0=19.28$ g/cm^3 and $\sigma=0.477$) and a light "particle" such as a bubble in fluid ($\rho_0=0$ and $\sigma=3$). The results of the numerical calculation of the velocity correlation function for these three cases are shown in Fig. 1. In the limit of $\sigma\to0$, Eq. (4) tends to Eq. (3), which is shown with the dotted line in Fig. 1. The lighter the Brownian particle and hence the larger the value of σ, the larger the deviation from the single exponential. In all the cases of $\sigma>0$, the velocity correlation function approaches

$$\langle u(0)u(t)\rangle\to\langle u^2\rangle(\sigma/2\pi^{1/2})(t/\tau)^{-3/2} \qquad (5)$$

in the time region much longer than τ. This is the long-time tail. The long-time tail was first observed by Alder and Wainright in their computer "experiment" of molecular dynamics.[1,2] Their numerical calculation revealed that the appearance of the
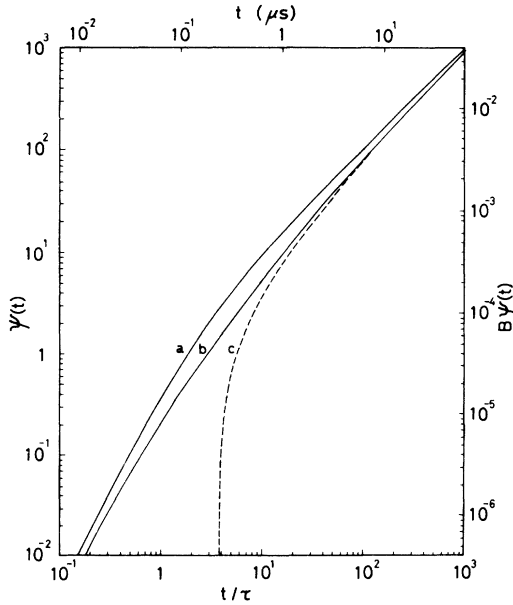
FIG. 2. Plots of $\psi(t)$ in the photon correlation function $g^{(2)}(t)=1+\exp[-B\psi(t)]$, where $B=2Dk_s^2t$. Lower horizontal axis represents the reduced time t/τ. Right-hand-side vertical axis and the upper horizontal axis represent, respectively, the value of $B\psi(t)$ and the actual time calculated for the light scattering from polystyrene latex spheres with a diameter of 0.804 μm suspended in water at 25 °C. Curve a, calculated with the Einstein-Stokes-type velocity correlation function; b, calculated with the Kubo-Widom-type velocity correlation function; c, long-time approximation $\psi(t)\simeq t/\tau-2\sigma(t/\pi\tau)^{1/2}$.

long-time tail could be explained in terms of the slowly developing viscous flow around a particle. The Brownian motion of the spherical particle described by the modified Langevin equation, Eq. (2), is a typical example showing such a long-time tail and is also a quite good system for the experimental test of the memory effect associated with non-Markovian nature of the stochastic process. Although the time dependence of the velocity correlation function changes largely depending on the value of σ, the diffusion coefficient D calculated from the velocity correlation function using the Green-Kubo formula[25] is independent of σ. Substitution of Eq. (4) in the formula yields

$$D=\int_0^\infty \langle u(0)u(t)\rangle dt = k_B T/6\pi a\eta .$$ (6)

This is just the relation derived by Einstein.[17] A direct dynamic measurement of the correlation function is, therefore, needed to test experimentally the

validity of the modified Langevin equation.

In this work, the photon correlation method was used to observe the Brownian motion of polystyrene latex spheres suspended in water. The method calculates the autocorrelation function of the scattered light intensity $I_s(t)$. Under ideal experimental conditions, we can observe the photon correlation function $g^{(2)}(t)=\langle I_s(0)I_s(t)\rangle/\langle I_s\rangle^2$, which is related to the velocity correlation function by[26]

$$g^{(2)}(t)=1+\exp[-B\psi(t)] ,$$ (7)

where $B=2Dk_s^2\tau$ and

$$\psi(t)=\tau^{-2}\int_0^t \phi(t')(t-t')dt' .$$ (8)

The scattering vector k_s is related to the scattering angle θ as

$$k_s=(4\pi n/\lambda)\sin(\theta/2) ,$$

where n is the refractive index of the sample and λ is the wavelength of the incident radiation. For the case of $\sigma=1.70$, the result of the calculation of $\psi(t)$ with the use of the Kubo-Widom-type velocity correlation function, Eq. (4), is shown in Fig. 2. Also shown in this figure is $\psi(t)$ for $\sigma=0$, which corresponds to the Einstein-Stokes-type velocity correlation function, Eq. (3). The difference between the two functions is large near $t/\tau=1$. The broken curve in Fig. 2 represents the approximation of $\psi(t)$ in the long-time region, which is written as

$$\psi(t)\rightarrow t/\tau-2\sigma(t/\pi\tau)^{1/2} .$$ (9)

The presence of the second term on the right-hand side of Eq. (9) is the memory effect related with the non-Markovian property of the Brownian motion.

III. EXPERIMENT

A. Apparatus

The experimental apparatus is schematically represented in Fig. 3. The light source was an Ar-ion laser operated at $\lambda=5145$ Å. The output power was usually controlled to 260 mW. The laser beam was focused with a lens of focal length $f=55$ cm. The diameter of the beam at the output of the laser was $D_l=1.5$ mm. The sample was set at the focal point of the lens and the approximate effective radius of the beam at the scattering volume was estimated as $\sigma_l\simeq2\lambda f/\pi D_l\simeq0.12$ mm. The light scattered at right angles was made to pass through two identical apertures. The aperture was square shaped with $d^2=0.45\times0.45$ mm^2. The separation of the two apertures was $L=62$ cm, which was long enough to satisfy the coherence condition

Sample Glass plate Lens

Ar-ion laser

Laser beam

Scattered light
(a)

— — Aperture 1

Photodiode

Laser beam

— — Aperture 2

Scattered light
(b)

Half mirror

PM 1 Amp 1

PM 2

Amp 2

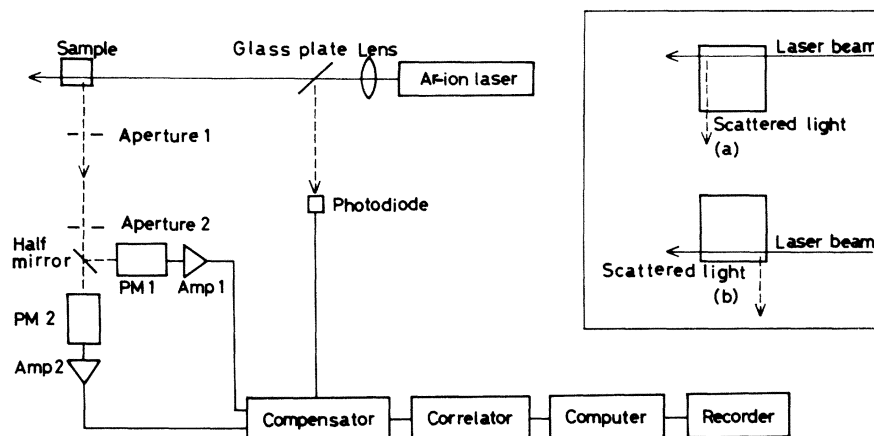Compensator — Correlator — Computer — Recorder

FIG. 3. Schematic illustration of the experimental apparatus. Two arrangements of the light scattering cell are shown in the inset. For details see the text.

$d^2/L < \lambda/n_0$, where n_0 is the refractive index of air. The actual scattering angle was determined to be $\theta = 90.0 \pm 0.2$ degrees from direct measurement of the arrangement of the optical assembly. The scattered light was divided with a half mirror and simultaneously detected with two separate photomultipliers, PM 1 and PM 2. The cross correlation between two signals from the two photomultipliers was measured. This procedure was used by Burnstyn et al. to eliminate correlation of the afterpulses from the photomultiplier.[27] A glass plate was used to reflect a part of the incident laser beam and to monitor the fluctuation of the laser light with a photodiode. The output of the photodiode was connected to a compensator, which is an electrical circuit to perform the division of the pulse density to compensate for a small intensity fluctuation of the laser light. The details of the circuit will be reported elsewhere.[28] The compensator also included a derandomizer which made the incident signal pulses synchronous to the clock pulses of the correlator.[29]

The correlator was the clipping type with one-bit (binary digit) shift registers as the delaying component.[29] The circuit constructions were similar to that reported before[30] but a few modifications were made. One is the addition of a circuit to determine the background of the correlation function. The main part of the correlator calculates the correlation function at 208 channels. The circuit was designed to delay the signal by 25 600 channels after the 208 channels and then to calculate the correlation function at an additional 16 channels for the determination of the background. The output of the correlator was connected to a NOVA3 minicomputer to analyze the data.

The temperature control was also a very important demand in this experiment. The temperature of the outer can of the sample holder assembly was controlled to $\pm 0.1\,^\circ\text{C}$ with the circulation of temperature-controlled water. The sample holder within the can was also temperature controlled with an electrical circuit. The circuit could control the temperature to $\pm 0.005\,^\circ\text{C}$ for one scan of about three hours. The measurements were repeated for about ten days and the temperature control for the total period was better than $\pm 0.02\,^\circ\text{C}$.

B. Sample

The polystyrene latex particles used as the sample were obtained from Dow Chemical Co. The catalog radius and the deviation are $a = 0.402$ μm and $\sigma_a = 0.0024$ μm, respectively. Dilute suspensions for the light scattering experiment were prepared from a stock suspension (10% solid) as follows.[31] A small amount of latex was diluted with freshly prepared deionized and double-distilled water in a glass centrifuge bottle of 40 cm^3 capacity to reduce the concentration to 7.0×10^{-3} g/cm^3. The dilute latex was then centrifuged at about 350 g for 25 min to remove larger aggregates. Further dilution was made to the concentration 3.6×10^{-6} g/cm^3 by adding double-distilled water. For this concentration, the mean distance between the particles was about 50 times as long as the particle diameter and the effect of the interaction between the particles is expected to be negligibly small. The sample cell used for the scattering was a cuboid of 10×10 mm^2 base and 50-mm height.

C. Procedure

For the sample investigated in this experiment, a numerical estimation gives $B = 4.032 \times 10^{-5}$ and $\tau = 6.246 \times 10^{-8}$ s at 25 °C. The actual time scale and the value of $B\psi(t)$ estimated are shown in Fig. 2. As already explained, the difference between the two correlation functions, Eq. (3) and Eq. (4), is very large in the time region $t = \sim\tau - 10\tau$. In this time region, $B\psi(t)$ is very small compared with unity, being of the order of $10^{-5} - 10^{-4}$. For $g^{(2)}(t)$ of Eq. (7), which is measured in the present experiment, the corresponding accuracy should be better than 10^{-6}. However, this accuracy is too high to be attained experimentally. In the time region longer than 3 μs, the value of $B\psi(t)$ is expected to become larger than 10^{-3}. Then we can work with an accuracy of the order of 10^{-4}, which is feasible. Also, in the time region longer than 6 μs, we can use the long-time approximation, Eq. (9), as shown in Fig. 2 with a broken line. This fact makes the least-squares data analysis very easy. From the above consideration, we chose the delay time per channel of the correlator as 6 μs. Having 208 channels in total, this measurement covered the time region 6 μs–1.2 ms.

Since the experiment should be done with high accuracy, we need to take into consideration all the possible experimental factors that might cause deformation of the correlation function. As such causes, we mention (i) output power fluctuation of

the laser, (ii) back reflection of the laser beam at the cell wall, (iii) after-pulsing of the photomultiplier, (iv) electronic distortion if any, (v) polydispersity of the polystyrene latex sphere, (vi) fluctuation of the sample temperature, (vii) vertical sedimentation motion of the particles in the gravitational field, (viii) number fluctuation of the particles within the scattering volume due to diffusion and sedimentation, (ix) multiple scattering, and (x) convective flow in the sample cell, if it exists.

As already explained, an electric circuit was used to compensate for the laser power fluctuation. The performance of the circuit was tested by observing the correlation function of the laser light reflected from the surface of a glass plate placed at the position of the sample cell. No correlation effect was observed within the accuracy of 10^{-4}. To avoid the back-reflection problem, we worked with the scattering only at right angles. In this case, the reflected beam also scatters light at right angles. The after-pulsing effect was eliminated by using two photomultipliers as shown in Fig. 3. We observed the correlation of the light emitted from an incandescent bulb powered with batteries. The correlation function was constant within the accuracy of 1×10^{-4}, which shows that the after-pulsing effect and the electronic distortion were absent. The effects from (v) to (viii) may be estimated by calculation. If we consider those effects, the correlation function of the scattered light may be written as

$$\langle I_s(0)I_s(t)\rangle = \gamma^2\langle N\rangle^2 + \gamma^2\langle N\rangle^2 A\exp\left[-Bt/\tau + 2\sigma B(t/\pi\tau)^{1/2} + \sum_{i=1}^{4} C_i(t)\right] + \gamma^2\langle N\rangle F_N(t). \tag{10}$$

Here $C_i(t)$'s are the correction terms given by

$$C_1(t) = 5B(\sigma_a/a)^2(t/\tau),$$

$$C_2(t) = B^2(\sigma_a/a)^2(t/\tau)^2/2,$$

$$C_3(t) = -B^2(\sigma_T/T)^2[1 - (T/\eta)(d\eta/dT)]^2 \times (t/\tau)^2/2,$$

$$C_4(t) = -v_s^2 t^2/\sigma_l^2,$$

where γ is a suitably chosen efficiency of the scattering and detection, $\langle N\rangle$ is the mean number of particles within the scattering volume, and A is a numerical factor related to the coherence, clipping, etc. The parameters σ_a, σ_l, and σ_T, are the mean deviation of the particle radius, the effective laser beam radius at the scattering volume, and the mean deviation of the sample temperature, respectively. Except for the correction terms $C_1(t) - C_4(t)$, Eq. (10) is the

ordinary formula of the photon correlation function.[26] The term $\gamma^2\langle N\rangle F_N(t)$ represents the number fluctuation. The corrections $C_1(t)$ and $C_2(t)$ correct the polydispersity of the latex spheres.[32] The effect of the temperature variation during the measurement is estimated by $C_3(t)$. This expression was derived by the approximation that the probability distribution of the temperature deviation ΔT from the mean value is Gaussian,

$$p(\Delta T) = (1/\sqrt{2\pi}\sigma_T)\exp(-\Delta T^2/2\sigma_T^2).$$

For the drift type of the temperature change, a different functional form is expected. However, the order of magnitude of the effect is estimated with this approximated form. The term $C_4(t)$ is the correction of the sedimentation during the measurement. The numerical estimations of these terms for the sample we used are $-Bt/\tau = -6.46 \times 10^2 t$,

TABLE I. Results of the least-squares-fit analysis of the observed photon correlation functions with the functional form $A' \exp(-p_1 t + p_{1/2} t^{1/2})$. rmsd indicates the root-mean-square deviation. Values in the parentheses are theoretically calculated values.

Temperature (°C)	p_1 (s^{-1})	$p_{1/2}$ (s$^{-1/2}$)	rmsd
32.8	760.58±0.18 (784.26)	0.397±0.015 (0.409)	3.972×10^{-4}
28.0	682.84±0.49 (697.35)	0.326±0.020 (0.346)	3.560×10^{-4}
23.5	610.49±0.43 (620.51)	0.267±0.017 (0.293)	3.280×10^{-4}

$2\sigma B(t/\pi\tau)^{1/2} = 3.05 \times 10^{-1} t^{1/2}$, $C_1(t) = 1.15 \times 10^{-1} t$, $C_2(t) = 7.42 t^2$, $C_3(t) = -2.95 \times 10^{-2} t^2$, and $C_4(t) = -3.04 \times 10^{-8} t^2$. These estimations were made for the temperature of 25 °C, by substituting the numerical values $\sigma_T = 0.02$ K and $\sigma_l = 0.012$ cm. The term $C_1(t)$ is a very small correction to the term Bt/τ. In the time region we are concerned about $(6 \times 10^{-6} - 1.3 \times 10^{-3}$ s), the correction $C_2(t)$ is at largest 0.7% of the $t^{1/2}$ term. The corrections

$C_3(t)$ and $C_4(t)$ are much smaller than $C_2(t)$. Thus we regard the t^2 correction terms as negligible in the data analysis.
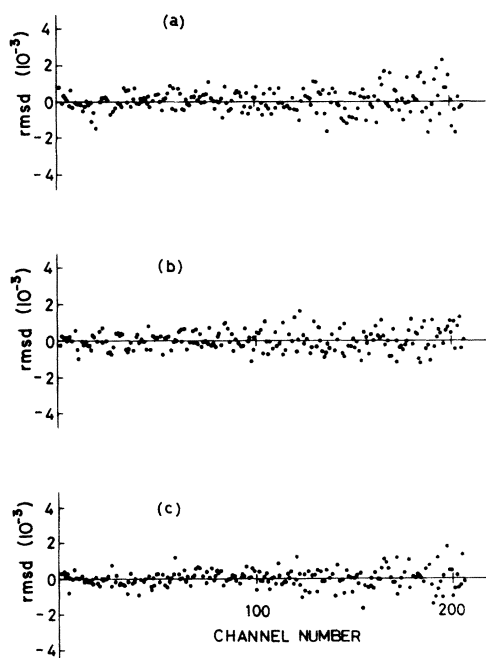
It is very difficult to estimate quantitatively the

FIG. 4. Deviation of the experimental values of the normalized photon correlation function from the best-fit function of the form $\exp(-p_1 t + p_{1/2} t^{1/2})$. No systematic deviation is observed. Temperatures are (a), 32.8 °C; (b), 28.0 °C; (c), 23.5 °C.
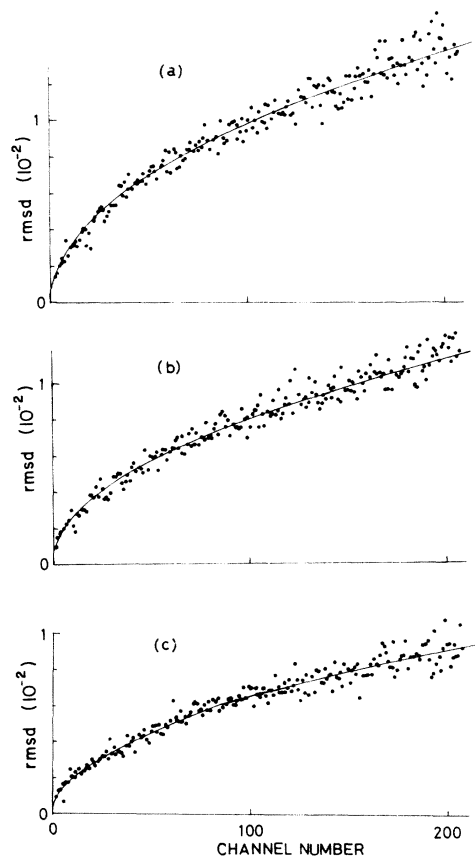
FIG. 5. Comparison of the best-fit value and the experimental value of the memory term $p_{1/2} t^{1/2}$ in the photon correlation function, which appears related to the non-Markovian nature of the Brownian motion. Temperatures are (a), 32.8 °C; (b), 28.0 °C; (c), 23.5 °C. For details see text.
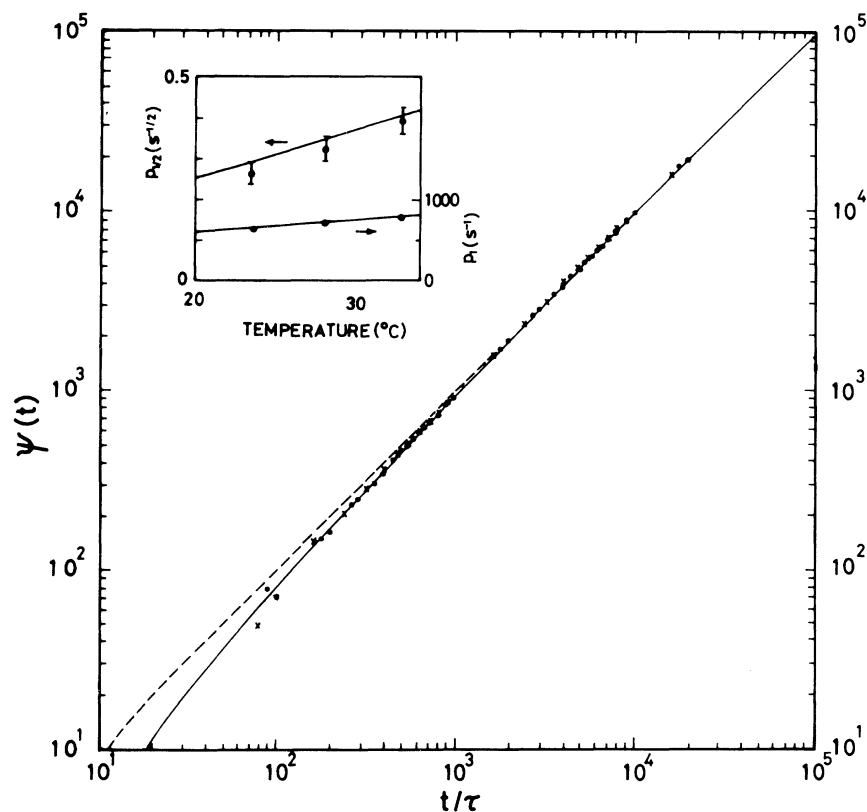
FIG. 6. Comparison of the experimental and calculated values of the function $\psi(t)$ defined by Eq. (8) in the text. Solid curve is calculated using the Kubo-Widom-type velocity correlation function and the broken line is calculated using the Einstein-Stokes-type velocity correlation function. Temperatures of the experimental points are $\times$, 32.8 °C; $\bigcirc$ 28.0 °C; and $\bullet$, 23.5 °C. All the experimental points at different temperatures lie on the curve calculated using the Kubo-Widom-type velocity correlation function. Inset shows comparison of the experimentally determined values of p_1 and $p_{1/2}$ with the theoretical calculations shown by the solid curves.

effect of multiple scattering. Therefore, in order to reduce the multiple scattering and also the interaction between particles, we diluted the sample density at a sacrifice of the data-acquisition time. We also tested the effect experimentally. For a particle having a diameter larger than the wavelength of light, the scattering is anisotropic, being stronger in the forward direction than in the backward direction. Then, if we observe the multiple scattering for the two different cases shown in the inset of Fig. 3, the multiple scattering will be much stronger in case a than in case b. If the data is affected by the multiple scattering, we will obtain different results for the two different cases of observation. We could detect no difference within the experimental accuracy. Thus, the multiple-scattering effect was expected to be small. The final data were taken with the b arrangement.

If there is a large temperature gradient within the sample, thermal convection might occur, and the direction and the magnitude of the convective flow would vary within the sample cell. Therefore, we would obtain different results for different positions of observation within the sample cell if the correlation function were affected by the convective flow. We could not detect any difference within the experimental accuracy. The laser beam might cause the local heating, but the data was found independent of the laser power up to 300 mW.

The subtraction of the dc term $\gamma^2\langle N \rangle^2$ and the number fluctuation term $\gamma^2\langle N \rangle F_N(t)$ from the observed correlation function $\langle I_s(0)I_s(t)\rangle$ was made after direct measurements of these terms. The relaxation time of the second term in Eq. (10) is τ/B, which is 1.55×10^{-3} s at 25 °C. The relaxation time τ_N of the number fluctuation is determined either by

sedimentation $\tau_N \simeq \sigma_l / v_s$ or by diffusion $\tau_N \simeq \sigma_l^2 / D$. The numerical values of those are estimated to be $\sigma_l / v_s \simeq 5.7 \times 10^3$ s and $\sigma_l^2 / D \simeq 2.4 \times 10^4$ s, respectively. Thus the sedimentation velocity v_s determines the number fluctuation relaxation in this case. As already explained, we measured the correlation function at 16 channels after $(208 + 25\,600)$ channels of delay. Because the delay time per channel was chosen to be 6 μs, the total delay time at those channels was $t_M = 1.55 \times 10^{-1}$ s. Under this condition, the second term in Eq. (10) is negligibly small because $t_M \simeq 100\tau / B$. In addition, since $t_M \simeq 4 \times 10^{-4} \tau_N$, the decay of the number fluctuation correlation function can be neglected in this time scale. Thus we can regard $\langle I_s(0) I_s(t) \rangle = \gamma^2 \langle N \rangle^2 + \gamma^2 \langle N \rangle F_N(0)$. Subtracting this value from the observed correlation function, we can estimate the second term in Eq. (10).

IV. RESULTS AND DISCUSSION

Measurements were made at temperatures 32.8 °C, 28.0 °C, and 23.5 °C, and the sample was newly prepared for each temperature. The data accumulation for one scan was continued until the number of counts at the first channel of the correlator exceeded about 10^7 counts. The scattered intensity was about 10^4 counts/s and it took longer than three hours for one scan. Ten such scans were repeated for each temperature. Then the sum of the ten scans was analyzed. The total number of counts at the first channel was about 10^8 and the statistical accuracy at this channel is expected to be 10^{-4}. The subtraction of the background made the accuracy worse. With the increase of the channel number the accuracy decreased further due to the decay of the correlation function. However, the result of the data analysis showed that the root-mean-square deviation was less than 4×10^{-4}, which was sufficiently small for the present purpose.

A least-squares-fit analysis was made to the functional form $A' \exp(-p_1 t + p_{1/2} t^{1/2})$ to determine A', p_1, and $p_{1/2}$ as adjustable parameters. Here $p_1 = B / \tau$ and $p_{1/2} = 2\sigma B / (\pi \tau)^{1/2}$. The results of B / τ and $2\sigma B / (\pi \tau)^{1/2}$ obtained are listed in Table I. The theoretical estimations are given in the parentheses. Although we note a deviation of a few percent of the experimental values from the theoretical estimations, the agreement is quite satisfactory. The temperature dependence of the experimental value is also consistent with theory. To show the deviation of the data from the fitted function, the data values were divided by the best-fit value of A' and the deviations from the best-fitted $\exp(-p_1 t + p_{1/2} t^{1/2})$ are plotted in Fig. 4. The division by A' means the normalization of the func-
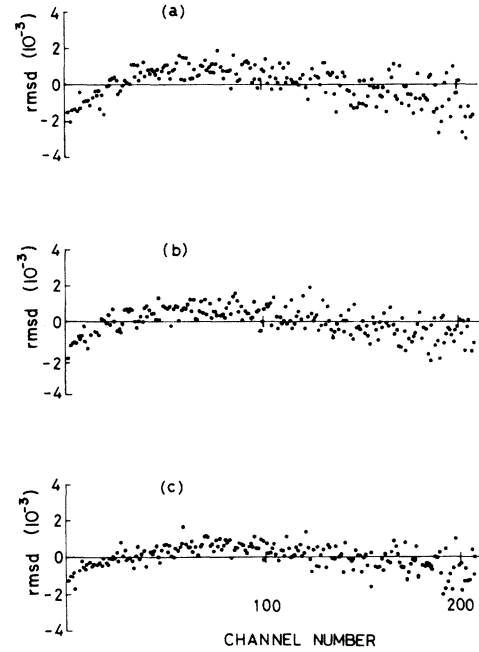

FIG. 7. Deviation of the experimental values of the normalized photon correlation function from the best-fit function of the form $\exp(-p_1 t)$. Systematic deviation is evident. Temperatures are (a), 32.8 °C; (b), 28.0 °C; (c), 23.5 °C.

tion to unity at $t = 0$. The plotted points in Fig. 4 show no systematic deviation. The scatter of the data is small enough to determine the magnitude of the $p_{1/2} t^{1/2} = 2\sigma B(t / \pi \tau)^{1/2}$ term. If we take the logarithm of the normalized data values and add the best-fit value of $p_1 t$ to them, the resultant values correspond to $p_{1/2} t^{1/2}$. In Fig. 5, these values are compared with the best-fit value of $p_{1/2} t^{1/2}$. The deviation is small compared with the change of $p_{1/2} t^{1/2}$. The best-fit values of B / τ and $2\sigma B / (\pi \tau)^{1/2}$ are compared with the theoretical values in the inset of Fig. 6 as a function of temperature. The error shown in Table I is estimated from the least-squares-fit analysis of the sum of the data of ten scans. We also analyzed each of the ten scans. The mean values agreed with the value shown in Table I. However, the root-mean-square deviations estimated from the best-fit values of the ten individual scans were a little larger than those listed in Table I. If we estimate the errors from the scatter of the results for different scans, the experimental values of $2\sigma B / (\pi \tau)^{1/2}$ are 0.397 ± 0.035 s$^{-1/2}$ at 32.8 °C, 0.326 ± 0.029 s$^{-1/2}$ at 28.0 °C, and 0.267 ± 0.027 s$^{-1/2}$ at 23.5 °C. The error bars shown

TABLE II. Results of the least-squares-fit analysis of the observed photon correlation functions with the functional form $A'\exp(-p_1 t)$. rmsd indicates the root-mean-square deviations.

Temperature (°C)	p_1 (s^{-1})	rmsd
32.8	750.77±0.71	6.335×10^{-4}
28.0	674.86±0.62	5.499×10^{-4}
23.5	604.03±0.54	4.786×10^{-4}

in the inset of Fig. 6 are estimated in this manner.

If we take the logarithm of the normalized data corresponding to $\exp[-Bt/\tau+2\sigma B(t/\pi\tau)^{1/2}]$ and then divide by $-p_1\tau=-B$, we get the experimental values corresponding to $\psi(t)$ defined by Eq. (8). For τ, calculated values were used. A comparison of the experimental values with the theoretical calculation is given in Fig. 6. The solid curve is the calculated function using the Kubo-Widom-type correlation function and the broken line is that using the Einstein-Stokes-type velocity correlation function. In showing that the experimental values at different temperatures lie on a single universal function, only part of the data points are displayed in order to eliminate overlap of the data points. It is clear that the experimental points obtained at different temperatures fit well to the single universal function calculated using the Kubo-Widom-type velocity correlation function for $\sigma=1.70$.

We also analyzed the data with the functional form $A'\exp(-p_1 t)$, which corresponds to the long-time approximation of the Einstein-Stokes-type correlation function. The results are shown in Table II and Fig. 7. Figure 7 shows the deviations of the normalized values from the best-fit values of $\exp(-p_1 t)$. Systematic deviations can be clearly seen. Corresponding to the increased deviations, an increase of the root-mean-square deviations are observed in Table II compared with the results shown in Table I. Thus we can claim that a clear departure

of the experimental values from the Einstein-Stokes-type correlation function was observed.

As shown in Eq. (10), a few effects cause the appearance of terms proportional to t^2. We showed by calculation that these effects are expected to be small. To check experimentally whether our data are affected by the presence of a t^2 term or not, we analyzed data with the function of the form $A'\exp(-p_1 t+p_{1/2}t^{1/2}+p_2 t^2)$. The results are listed in Table III. We observe small variation of the values of B/τ and $2\sigma B/(\pi\tau)^{1/2}$ compared with those listed in Table I. The contribution from the term $p_2 t^2$ seems to be too small to be consistently determined from the present experiment. In fact, the change of p_2 with the temperature is not systematic: it is negative at 32.8 °C and 23.5 °C, and positive at 28.0 °C. Although we cannot fully deny the possibility of the small effect due to the t^2 term from the present experimental results only, we can at least claim from the results shown in Table III that the data are not largely affected by the presence of t^2 terms.

From the above discussion, we believe that the values given in Table I and Fig. 6 are appropriately estimated from the present experiment. As a quantitative result to be compared with the present result, we can only mention the work done by Paul and Pussey.[15] The value they got was (74±3)% of the value predicted theoretically, but we do not find such a large departure. All the mean values we obtain are slightly smaller than the value predicted theoretically. However, the deviations are less than 10%. The small systematic deviation may be explained either by a deviation of a few percent of the physical parameters we used for the calculation from the real values or by the presence of a small uncontrolled experimental artifact that might cause the deformation of the correlation function. The temperature dependence of our data is consistent with the theoretical prediction as shown in Fig. 6. This fact is strong experimental support of the correctness of Eq. (4) in describing the non-

TABLE III. Results of the least-squares-fit analysis of the observed photon correlation functions with the functional form $A'\exp(-p_1 t+p_{1/2}t^{1/2}+p_2 t^2)$. rmsd indicates the root-mean-square deviation.

Temperature (°C)	p_1 (s^{-1})	$p_{1/2}$ (s$^{-1/2}$)	p_2 (s^{-2})	rmsd
32.8	758.24±0.17	0.345±0.012	$(-0.976\pm0.405)\times10^3$	3.970×10^{-4}
28.0	683.02±0.15	0.330±0.011	$(0.691\pm3.66)\times10^3$	3.599×10^{-4}
23.5	607.07±0.12	0.190±0.010	$(-1.39\pm0.33)\times10^3$	3.252×10^{-4}

Markovian Brownian motion of spherical particles suspended in water.

ACKNOWLEDGMENTS

[1]B. Alder and T. Wainright, Phys. Rev. Lett. 18, 988 (1967); Phys. Rev. A 1, 18 (1970).

[2]B. Alder, T. Wainright, and D. Gass, Phys. Rev. A 4, 233 (1971).

[3]For a review, see Y. Pomeau and P. Résibois, Phys. Rep. 19C, 63 (1975).

[4]R. Zwanzig and M. Bixon, Phys. Rev. A 2, 2005 (1970).

[5]A. Widom, Phys. Rev. A 3, 1394 (1971).

[6]R. Kubo, Rep. Prog. Phys. 29, 235 (1966).

[7]C. D. Andriesse, Phys. Lett. 33A, 419 (1970).

[8]K. Carneiro, Phys. Rev. A 14, 517 (1976).

[9]J. Bosse, W. Gotze. and M. Lucke, Phys. Rev. A 20, 1603 (1979).

[10]Y. W. Kim and J. E. Matta, Phys. Rev. Lett. 31, 208 (1973).

[11]P. D. Fedele and Y. W. Kim, Phys. Rev. Lett. 44, 691 (1980).

[12]S. Harris, Phys. Lett. 47A, 77 (1974).

[13]J. P. Boon and A. Bouiller, Phys. Lett. 55A, 391 (1976).

[14]A. Bouiller, J. P. Boon, and P. Deguent, J. Phys. (Paris) 39, 159 (1978).

[15]G. L. Paul and P. N. Pussey, J. Phys. A 14, 3301 (1981).

[16]G. E. Uhlenbeck and L. S. Onsager, Phys. Rev. 36, 823 (1930).

[17]A. Einstein, Investigation on the Theory of the Brownian Motion (Dover, New York, 1956).

[18]L. D. Landau and E. M. Lifshitz, Fluid Mechanics (Addison-Wesley, Reading, Mass., 1959), Chap. 2.

[19]P. Mazur and D. Bedeaux, Physica (Utrecht) 76, 235 (1974).

[20]R. Zwanzig and M. Bixon, J. Fluid Mech. 69, 21 (1975).

[21]E. Hinch, J. Fluid Mech. 72, 499 (1975).

[22]R. Kubo, Rep. Res. Inst. Math. Sci. (Kyoto University) 367, 50 (1979); private memorandum.

[23]M. Warner, J. Phys. A 12, 1511 (1979).

[24]R. B. Jones, Physica (Utrecht) 101A, 389 (1980).

[25]R. Zwanzig, Ann. Rev. Phys. Chem. 61, 670 (1965).

[26]B. J. Berne and R. Pecora, Dynamic Light Scattering (Wiley, New York, 1976).

[27]H. C. Burnstyn, F. C. Chang, and J. V. Sengers, Phys. Rev. Lett. 44, 410 (1980).

[28]G. Terui, T. Kohno, Y. Fukino, and K. Ohbayashi (unpublished).

[29]Photon Correlation and Light Beating Spectroscopy, edited by H. Z. Cummins and E. R. Pike (Plenum, New York, 1974).

[30]K. Ohbayashi, Jpn. J. Appl. Phys. 13, 1219 (1974).

[31]W. Heller and R. J. Tabibian, J. Phys. Chem. 66, 2059 (1962).

[32]S. P. Lee, W. Tshaunuter, and B. Chu, J. Polym. Sci. 10, 2453 (1972).